

Ca²⁺ Release via IP₃ Receptors Shapes the Cardiac Ca²⁺ Transient for Hypertrophic Signaling

Hilary Hunt,¹ Agn e Tilunait e,¹ Greg Bass,¹ Christian Soeller,² H. Llewelyn Roderick,³ Vijay Rajagopal,^{4,*} and Edmund J. Crampin^{1,5,*}

¹Systems Biology Laboratory, School of Mathematics and Statistics and Melbourne School of Engineering, University of Melbourne, Melbourne, Australia; ²Living Systems Institute, University of Exeter, Exeter, United Kingdom; ³Laboratory of Experimental Cardiology, Department of Cardiovascular Sciences, KU Leuven, Belgium; ⁴Cell Structure and Mechanobiology Group, Department of Biomedical Engineering, Melbourne School of Engineering and ⁵ARC Centre of Excellence in Convergent Bio-Nano Science and Technology, School of Chemical and Biomedical Engineering, University of Melbourne, Melbourne, Australia

ABSTRACT Calcium (Ca²⁺) plays a central role in mediating both contractile function and hypertrophic signaling in ventricular cardiomyocytes. L-type Ca²⁺ channels trigger release of Ca²⁺ from ryanodine receptors for cellular contraction, whereas signaling downstream of G-protein-coupled receptors stimulates Ca²⁺ release via inositol 1,4,5-trisphosphate receptors (IP₃Rs), engaging hypertrophic signaling pathways. Modulation of the amplitude, duration, and duty cycle of the cytosolic Ca²⁺ contraction signal and spatial localization have all been proposed to encode this hypertrophic signal. Given current knowledge of IP₃Rs, we develop a model describing the effect of functional interaction (cross talk) between ryanodine receptor and IP₃R channels on the Ca²⁺ transient and examine the sensitivity of the Ca²⁺ transient shape to properties of IP₃R activation. A key result of our study is that IP₃R activation increases Ca²⁺ transient duration for a broad range of IP₃R properties, but the effect of IP₃R activation on Ca²⁺ transient amplitude is dependent on IP₃ concentration. Furthermore we demonstrate that IP₃-mediated Ca²⁺ release in the cytosol increases the duty cycle of the Ca²⁺ transient, the fraction of the cycle for which [Ca²⁺] is elevated, across a broad range of parameter values and IP₃ concentrations. When coupled to a model of downstream transcription factor (NFAT) activation, we demonstrate that there is a high correspondence between the Ca²⁺ transient duty cycle and the proportion of activated NFAT in the nucleus. These findings suggest increased cytosolic Ca²⁺ duty cycle as a plausible mechanism for IP₃-dependent hypertrophic signaling via Ca²⁺-sensitive transcription factors such as NFAT in ventricular cardiomyocytes.

SIGNIFICANCE Many studies have identified a role for inositol 1,4,5-trisphosphate receptor (IP₃R)-mediated Ca²⁺ signaling in cardiac hypertrophy; however, the signaling mechanism remains unclear. Here we present a mathematical model of functional interactions between ryanodine receptors (RyRs) and IP₃Rs, and show that IP₃-mediated Ca²⁺ release can increase the Ca²⁺ duty cycle, which has been shown experimentally to lead to NFAT activation and hypertrophic signaling. Through a parameter sensitivity analysis, we demonstrate that the duty cycle increases with IP₃ over a broad parameter regime, indicating that this mechanism is robust, and furthermore we show that increasing Ca²⁺ duty cycle raises nuclear NFAT activation. These findings suggest a plausible mechanism for IP₃R-dependent hypertrophic signaling in cardiomyocytes.

INTRODUCTION

Calcium is a universal second messenger that plays a role in controlling many cellular processes across a wide variety of

cell types, ranging from fertilization, cell contraction, and cell growth to cell death (1,2). Precisely how Ca²⁺ fulfills each of these roles while also ensuring signal specificity remains unclear in many cases. Ca²⁺ can be used to transmit signals in a variety of ways. Signal localization and amplitude and frequency modulation have been widely explored (3–5); however, mechanisms for information encoding in the cumulative signal (i.e., area under the curve, proportional-integral-derivative controller, or duty cycle) have also been proposed (6–8). Determining which method of information encoding is relevant to a specific signaling

Submitted January 24, 2020, and accepted for publication August 4, 2020.

*Correspondence: vijay.rajagopal@unimelb.edu.au or edmund.crampin@unimelb.edu.au

Vijay Rajagopal and Edmund J. Crampin contributed equally to the supervision of this work.

Editor: Eric Sobie.

<https://doi.org/10.1016/j.bpj.2020.08.001>

  2020 Biophysical Society.

pathway requires determining what type of signal encoding the system is capable of and whether the downstream effector of the signal is capable of temporal signal integration, high- or low-pass filtering, or threshold filtering.

In cardiac myocytes, discrete encoding of multiple Ca²⁺-mediated signals is particularly pertinent because of the essential and continuous role Ca²⁺ plays in excitation-contraction coupling (ECC). Of particular significance is the involvement of Ca²⁺ in hypertrophic growth signaling. How Ca²⁺ can communicate a signal in the hypertrophic signaling pathway concurrent with the cytosolic Ca²⁺ fluxes that drive cardiac muscle contraction is still largely unresolved (9,10). Understanding this mechanism is important because pathological hypertrophic remodeling is a precursor of heart failure and a common final pathway of cardiovascular diseases, including hypertension and coronary disease (11–13).

During each heartbeat, on depolarization of the membrane Ca²⁺ enters the cell via L-type Ca²⁺ channels (LTCCs), triggering larger Ca²⁺ release from the sarcoplasmic reticulum (SR) via ryanodine receptors (RyRs), which then induces contraction. The activation of Ca²⁺ release via RyRs by the Ca²⁺ arising via LTCCs is known as calcium-induced calcium release and results in a 10-fold increase in cytosolic Ca²⁺ concentration (relative to resting Ca²⁺ concentration of ~100 nM). Sarcoplasmic reticulum Ca²⁺ pumps (SERCA) and other Ca²⁺ sequestration mechanisms subsequently withdraw the released Ca²⁺ back into the SR and out of the cytosol (14,15), reverting

the cell to its relaxed state. Ca²⁺ also plays a central role in hypertrophic signaling. Hypertrophic stimuli such as endothelin-1 (ET-1) bind to G-protein-coupled receptors at the cell membrane to stimulate generation of the intracellular signaling molecule inositol 1,4,5-trisphosphate (IP₃). After IP₃ binds to and activates its cognate receptor, inositol 1,4,5-trisphosphate receptors (IP₃R), on the SR and nuclear envelope, Ca²⁺ is released into the cytosol and nucleus, respectively (see Fig. 1; (16,17)). This Ca²⁺ signal arising from IP₃R has been shown in multiple mammalian species to produce a distinct Ca²⁺ signal that through activation of pro-hypertrophic pathways, including those involving nuclear factor of activated T cells (NFAT), induces hypertrophy within cardiomyocytes (16,18,19).

In healthy adult rat ventricular myocytes (ARVMs), various effects of IP₃ on global Ca²⁺ transients associated with ECC have been described, summarized in Table 1. Although application of G-protein-coupled receptor agonists that stimulate IP₃ generation produces robust effects on ECC-associated IP₃ transients and contraction, the direct contribution of IP₃ to these actions varies between studies (17,20–24). For example, in rabbits the effect of ET-1 on Ca²⁺ transient amplitude is sensitive to the IP₃R inhibitor 2-APB (22), whereas in healthy rats, IP₃R inhibition with 2-APB was without effect (25). In mice, 2-APB abrogated an increase in ECC-associated Ca²⁺ transients brought about by AngII (24). Responses have also been variable when IP₃ was directly applied to cardiac myocytes. In healthy rats, IP₃ produced no or a modest effect on Ca²⁺

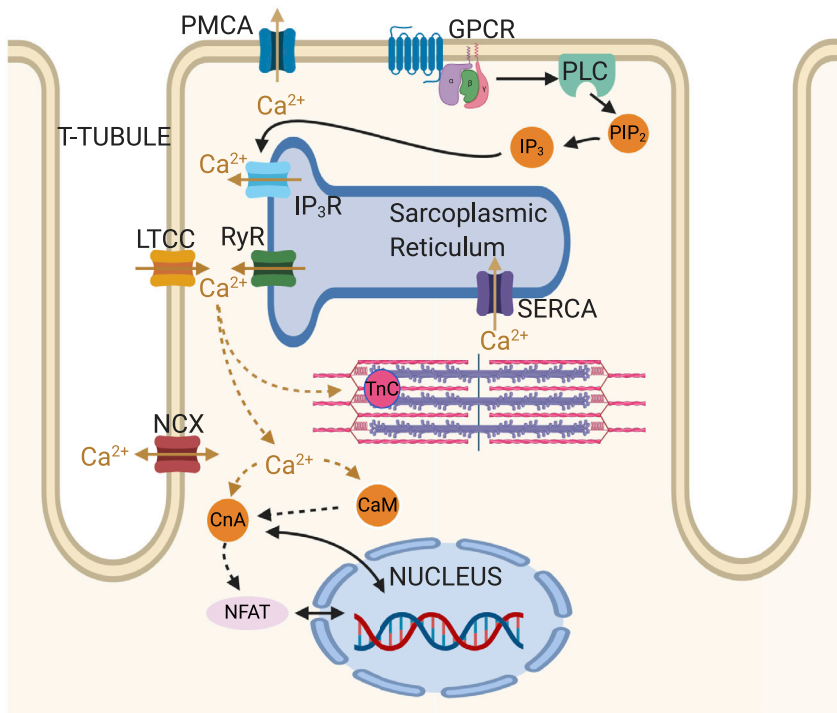


FIGURE 1 Schematic showing key Ca²⁺ signaling pathways in the cardiomyocyte. ECC processes include ryanodine receptors (RyRs), L-type Ca²⁺ channels (LTCCs), SERCA, sodium-calcium exchanger (NCX), sarcolemmal calcium pump (PMCA), and troponin C (TnC). Growth-related IP₃-Ca²⁺/NFAT signaling processes include inositol 1,4,5-trisphosphate receptors (IP₃R), G-protein-coupled receptor (GPCR), phospholipase C (PLC), phosphatidylinositol 4,5-bisphosphate (PIP₂), calmodulin (CaM), calcineurin (CnA), and nuclear factor of activated T cells (NFAT). To see this figure in color, go online.

TABLE 1 Summary of Experimentally Observed Changes to the Ca²⁺ Transient in Normal Healthy Ventricular Myocytes in Rat and Other Species after Addition of IP₃ and ET-1

Cell State		IP ₃	ET-1
Rat	Amplitude:	r▲(21) r◆(17)	r▲(21) r◆(16) r▲(17)
	Duration:	–	–
	Basal Ca ²⁺ :	r◆(17)	r◆(17)
	SCTs:	r▲(21) r▲(17)	r▲(21) r▲(17)
Other species	Amplitude:	m▲(20) m◆(73)	h▲(20) m▲(20)
	Duration:	–	–
	Basal Ca ²⁺ :	m▲(73)	m▲(20), b▲(22)
	SCTs:	–	h▲(20) m▲(20)

SCT, spontaneous Ca²⁺ transient. ▲ indicates an increase, ▼ a decrease, and ◆ indicates no significant change reported; r indicates rat, b indicates rabbit, h indicates human, and m indicates mouse; dashes indicate no data found. The model developed in this work is primarily parameterized with rat data.

transient amplitude (17,21), whereas in rabbits (22), a more substantial effect was observed. These differences in the effect of IP₃ have been ascribed in part to the greater dependence of rat myocytes on SR Ca²⁺ release to the Ca²⁺ transient than rabbit myocytes (22). Notably, both ET-1 and IP₃ elicit arrhythmogenic effects whereby they promote the generation of spontaneous calcium transients, manifest as a prolonged Ca²⁺ transient with additional peaks, and increase the frequency of Ca²⁺ sparks (17,18,21,22). A more profound role for IP₃ signaling is observed in hypertrophic ventricular myocytes, with ECC-associated Ca²⁺ transients of greater amplitude reported. Underlying these effects, IP₃R expression is elevated in hypertrophy (26). Hence, a question remains as to what independent effect IP₃R activation has on the cytosolic Ca²⁺ transient in healthy ventricular cardiac myocytes.

The individual behavior of IP₃R channels and their dependence on Ca²⁺, IP₃, and ATP in cardiac and other cell types has been explored in a number of studies (27–30). These studies have formed the basis of several computational models of IP₃R type I isoforms (29,31,32) fitted to stochastic single-channel data (33). However, properties of IP₃R channel activity within the cardiomyocyte, such as gating state transition rates and their dependency on IP₃ and Ca²⁺, have not been directly measured. In this study, we have taken the experimental studies on rat ventricular cardiomyocytes as a reference point for the observed effects of IP₃R activation on cellular Ca²⁺ dynamics and extended a well-established model of beat-to-beat cytosolic Ca²⁺ transients in rat cardiac cells (14,34) to include a model of type II IP₃R (32) channels. This deterministic, compartmental model of ECC enables us to investigate biophysically plausible mechanisms by which IP₃R activation could affect Ca²⁺ dynamics at the whole-cell scale while avoiding the computational complexity associated with detailed stochastic and spatial modeling. Specifically, it enables us to explore the parameter ranges of IP₃R-mediated Ca²⁺ release that modify the global cytosolic Ca²⁺ transient to encode information for hypertrophic signaling to the nucleus.

A number of transcription factors transduce changes in Ca²⁺ to activate hypertrophic gene transcription. Of particular note is NFAT. There are five known NFAT isoforms ex-

pressed in mammals; four of these are found in cardiac cells (19,35). To initiate hypertrophic remodeling, the hypertrophic Ca²⁺ signal, in conjunction with calmodulin (CaM) and calcineurin (CaN), leads to dephosphorylation of cytosolic NFAT. Upon dephosphorylation, NFAT translocates to the nucleus, where, in coordination with other proteins, it activates expression of genes responsible for hypertrophy (36). Several studies have focused on characterizing the Ca²⁺ dynamics necessary to activate NFAT and initiate hypertrophy (8,19,37–42) and have shown NFAT to be a Ca²⁺ signal integrator (37). Furthermore, a recent study by Hannanta-anan and Chow (8) used direct optogenetic control of cytosolic Ca²⁺ transients in HeLa cells to demonstrate that the transcriptional activity of NFAT4 (also known as NFATc3), a necessary NFAT isoform in the hypertrophic pathway (35), can be upregulated by increasing the residence time of Ca²⁺ in the cytosol within each oscillation. The increased residence time of Ca²⁺, referred to as the “duty cycle,” is the ratio between the area under the Ca²⁺ transient curve divided by the maximal possible area, as calculated by the product of transient amplitude and period (see Fig. 2A). The Ca²⁺ duty cycle is therefore distinct from the average Ca²⁺ concentration. Hannanta-anan and Chow (8) showed that increasing the duty cycle had a proportionally greater effect on NFAT transcriptional activity than changing either the frequency or amplitude of the cytosolic Ca²⁺ oscillations. This suggests an increased Ca²⁺ duty cycle as a possible mechanism by which Ca²⁺ release through IP₃R channels can affect hypertrophic signaling.

Here, using a mathematical model of beat-to-beat cytosolic Ca²⁺ transients in rat ventricular myocytes, coupled to IP₃R channel Ca²⁺ release, we show that IP₃R activation in the cytosol can increase the duty cycle of the cytosolic Ca²⁺ transient. We establish model feasibility through parameter sensitivity analysis, which shows that this behavior does not depend sensitively on model parameter values. Furthermore, we identify conditions necessary for IP₃R channel activation to alter Ca²⁺ transient amplitude, width, basal Ca²⁺, and duty cycle, as identified in different experimental studies, and compare model simulations to published experimental data summarized in Table 1. Finally, we couple simulations of cytosolic Ca²⁺ dynamics to a

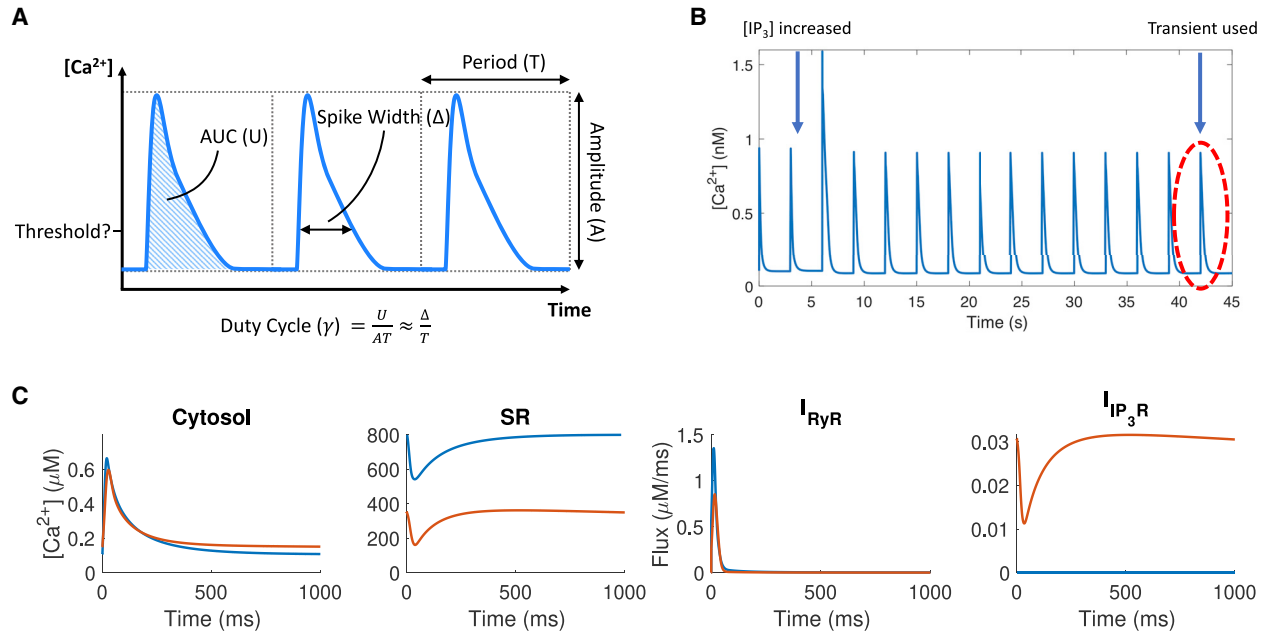


FIGURE 2 (A) The duty cycle, a function of area under the curve, amplitude, and period, for the cytosolic Ca^{2+} transient. (B) An example of Ca^{2+} transients generated by the model is shown. (C) Ca^{2+} concentration in cytosol and SR, RyR flux, and IP₃R flux in the model with elevated IP₃ (red) and without IP₃ (blue) are shown. Here, IP₃R parameters used are taken from (32), with maximal IP₃R flux $k_f = 0.003 \mu\text{M}^3 \text{ms}^{-1}$. To see this figure in color, go online.

model of downstream CaM/CnA/NFAT activation and show that the duty cycle of the Ca^{2+} transient highly correlates with the activated nuclear NFAT (the proportion of NFAT that is dephosphorylated and translocated to the nucleus). These findings suggest IP₃R activity can increase the cytosolic Ca^{2+} duty cycle, thus providing a mechanism for IP₃-dependent activation of NFAT for hypertrophic signaling in the cardiomyocyte.

METHODS

We developed a computational model of RyR- and IP₃R-mediated Ca^{2+} fluxes in the adult rat ventricular myocyte. Model simulations were performed using the ode15s ODE solver from MATLAB 2017b (The MathWorks, Natick, MA) with relative and absolute tolerances 1×10^{-3} and 1×10^{-6} , respectively. The model equations were simulated at 1 Hz, the original pacing frequency of the Hinch et al. (14) model, and at 0.3 Hz because it is another common pacing frequency in experimental studies of IP₃ and Ca^{2+} in cardiomyocytes (17,21). The model was paced until the normalized root mean-square deviation between each subsequent beat was below 1×10^{-3} , and all but the last oscillation were discarded to eliminate transient behaviors (see Fig. 2 B). Initial conditions were set to the basal Ca^{2+} level of the model at dynamic equilibrium with inactive IP₃R channels, determined after running the base model until the normalized root mean-square deviation was also below 1×10^{-3} .

Model equations

The compartmental model of rat left ventricular cardiac myocyte Ca^{2+} dynamics is based on the Hinch et al. (14) model of ECC, with the addition of IP₃R Ca^{2+} release modeled using the Siekmann-Cao-Sneyd model (32). The Hinch model is an established whole-cell model of rat cardiac Ca^{2+} dynamics that describes the flux through the major Ca^{2+} channels and

pumps on the cell and SR membranes and the effects of applying a voltage across the cell membrane. The parameters for the Hinch component of our model were maintained from the original, except for those of the driving voltage. This was shortened to better approximate the rat action potential (43) (see Fig. S1). The Ca^{2+} in the cytosol is governed by the following ODE:

$$\frac{d[\text{Ca}^{2+}]_{\text{cyt}}}{dt} = \beta_{\text{fluo}} \times \beta_{\text{CaM}} \times (I_{\text{CaL}} + I_{\text{RyR}} - I_{\text{SERCA}} + I_{\text{IP}_3\text{R}} + I_{\text{other}}), \quad (1)$$

$$I_{\text{other}} = I_{\text{SR1}} + I_{\text{NCX}} - I_{\text{PMCA}} + I_{\text{CaB}} + I_{\text{TnC}}. \quad (2)$$

A small Ca^{2+} flux through the LTCCs, I_{CaL} , activates RyR channels to release Ca^{2+} from the SR into the cytosol at a rate of I_{RyR} . Ca^{2+} is resequenced into the SR by SERCA at a rate I_{SERCA} . β_{fluo} is the rapid buffer coefficient (44) for the fluorescent dye in the cytosol, and β_{CaM} is the rapid buffer coefficient for calmodulin in the cytosol. I_{other} includes Ca^{2+} fluxes such as exchange with the extracellular environment through the sodium-calcium exchanger I_{NCX} , sarcolemmal Ca^{2+} -ATPase I_{PMCA} , and the background leak current I_{CaB} , as well as the SR leak current I_{SR1} and buffering on troponin C I_{TnC} . These fluxes are defined in the Supporting Materials and Methods.

When the simulation is run with IP₃ present, there is additionally a flux through the IP₃Rs:

$$I_{\text{IP}_3\text{R}} = k_f \times N_{\text{IP}_3\text{R}} \times P_{\text{IP}_3\text{R}} \times \left([\text{Ca}^{2+}]_{\text{SR}} - [\text{Ca}^{2+}]_{\text{cyt}} \right) / V_{\text{myo}}. \quad (3)$$

Here, V_{myo} is the volume of the cell. k_f is the maximal total flux through each IP₃R channel; this was chosen to be $0.45 \mu\text{M}^3 \text{ms}^{-1}$ unless otherwise stated to create a measurable effect on IP₃R channel activation while

maintaining plausible total flux. N_{IP_3R} is the number of IP₃R channels in the cell; this was set to 1/50th of the number of RyR channels (45). We studied the effect of varying k_f on IP₃-induced changes to the cytosolic Ca²⁺ transient in normal cardiomyocytes. Evidently, varying N_{IP_3R} and varying k_f have the same effect on simulated calcium dynamics. Although N_{IP_3R} is known to increase significantly in disease conditions, we have not emphasized it in this study because of our focus on normal cardiomyocytes. $[Ca^{2+}]_{cvt}$ and $[Ca^{2+}]_{SR}$ are the Ca²⁺ concentrations in the cytosol and SR, respectively.

P_{IP_3R} is the $[Ca^{2+}]$ - and $[IP_3]$ -dependent open probability of the IP₃R channels and is determined using the Siekmann-Cao-Sneyd model (31,32,46), which has a built-in delay in response to changing Ca²⁺ concentration, along with several parameters governing channel activation and inactivation. This model describes P_{IP_3R} as

$$P_{IP_3R} = \beta / (\beta + k_\beta \times (\beta + \alpha)), \quad (4)$$

where k_β is a transition term derived from single-channel Siekmann et al. (46) and β describes the rate of activation and α the rate of inactivation:

$$\beta = B \times m \times h, \quad (5)$$

$$\alpha = (1 - B) \times (1 - m \times h_\infty), \quad (6)$$

where h is time dependent and B , m , and h and h_∞ describe the dependence on IP₃, the dependence on Ca²⁺, and the Ca²⁺-dependent delay in IP₃R gating, respectively. Expressions for these variables are as follows:

$$B = [IP_3]^2 / (K_p^2 + [IP_3]^2), \quad (7)$$

$$m = [Ca^{2+}]^4 / (K_c^4 + [Ca^{2+}]^4), \quad (8)$$

$$\frac{dh}{dt} = ((h_\infty - h) \times (K_t^4 + [Ca^{2+}]^4)) / (t_{max} \times K_t^4), \quad (9)$$

$$h_\infty = K_h^4 / (K_h^4 + [Ca^{2+}]^4). \quad (10)$$

Here, K_c and K_h are parameters that determine the Ca²⁺-dependence of IP₃R channel open probability, whereas K_t and t_{max} are parameters that affect the delay in IP₃R response to cytosolic changes. K_t determines the influence of $[Ca^{2+}]$ on the delay, whereas t_{max} is a temporal scaling factor.

We note that the SR leak flux, I_{SR1} , is unchanged from the Hinch model and would include the effects of diastolic IP₃R Ca²⁺ release at normal IP₃ levels because that model did not explicitly include IP₃R. However, in the presence of IP₃, IP₃R Ca²⁺ flux during diastole is several orders of magnitude greater than I_{SR1} , which is largely dependent on $[Ca^{2+}]_{SR}$, and hence, any discrepancy caused by this will have a negligible effect on overall Ca²⁺ dynamics within the cell (see also Fig. S4).

Several experimental studies have investigated IP₃R activity across a range of Ca²⁺ concentrations with 1 μ M IP₃ (27,47). These studies suggest that IP₃R channels would be open, with almost constant P_{IP_3R} over the full range of cytosolic Ca²⁺ concentrations experienced during ECC in the cardiomyocyte. An IP₃R-facilitated SR-Ca²⁺ leak has been reported to amplify systolic concentrations (48,49), as seen in most published experiments of IP₃-enhanced Ca²⁺ transients tabulated in Table 1. Through parameter sensitivity analysis of this model, we show that to be consistent with these observations, P_{IP_3R} must be significantly smaller at resting Ca²⁺ concentrations than at higher concentrations.

Coupling cytosolic Ca²⁺ and NFAT activation

We coupled the calcium model to the NFAT model developed by Cooling et al. (50), which determines the proportion of total cellular NFAT that is dephosphorylated and translocated to the nucleus for a given cytosolic Ca²⁺ signal. In this study, we have used the model parameters estimated from the data in Tomida et al. (37), who measured activation of NFAT4 in BHK cells. Full details of the Cooling et al. (50) model are given in the Supporting Materials and Methods.

RESULTS

An example of the model output when run with the original IP₃R channel parameter values determined by Sneyd et al. (32) for type I IP₃R channels is shown in Fig. 2 C. Measurements of the properties of IP₃R channel activity and their dependence on Ca²⁺ within cardiomyocytes are sparse in the literature. Therefore, we performed a parameter sensitivity analysis by running model simulations over a variety of parameter ranges to explore the dependence of features of the cytosolic calcium transient to IP₃R channel parameters.

Parameter sensitivity analysis

We conducted a parameter sensitivity analysis to determine the critical parameters related to IP₃R activation that affect the shape of beat-to-beat cytosolic Ca²⁺ transients. We used the Jansen method (51) as described in Saltelli et al. (52) (and summarized in the Supporting Materials and Methods) to calculate the “main effect” and “total effect” coefficients of each of the parameters associated with IP₃R channel gating in relation to changes in transient amplitude, full duration at half maximum (FDHM), diastolic Ca²⁺, and duty cycle (see Table 2). Saltelli et al. (52) describe the main effect coefficient as “the expected reduction in variance that would be obtained if [the parameter] could be fixed” and the total effect coefficient as “the expected variance that would be left if all factors but [the parameter]

TABLE 2 Main and Total Effects of the IP₃R Gating Parameters on Ca²⁺ Transient Amplitude, Duration, Diastolic Ca²⁺, and Duty Cycle

Main Effect Coefficients	[IP ₃]	t_{max}	K_c	K_h	K_t	k_f
Amplitude	0.27 ^a	0.00	0.03	0.19 ^a	0.00	0.03
Duration (FDHM)	0.17 ^a	0.00	0.01	0.12 ^a	0.00	0.50 ^a
Diastolic Ca ²⁺	0.44 ^a	0.00	0.09	0.03	0.00	0.04
Duty cycle	0.23 ^a	0.00	0.01	0.16 ^a	0.00	0.33 ^a
Total Effect Coefficients	[IP ₃]	t_{max}	K_c	K_h	K_t	k_f
Amplitude	0.63 ^a	0.04	0.43 ^a	0.46 ^a	0.02	0.13 ^a
Duration (FDHM)	0.33 ^a	0.00	0.19 ^a	0.19 ^a	0.00	0.54 ^a
Diastolic Ca ²⁺	0.79 ^a	0.00	0.45 ^a	0.06	0.00	0.18 ^a
Duty cycle	0.45 ^a	0.00	0.25 ^a	0.24 ^a	0.00	0.38 ^a

Duration measured in FDHM.

^aSignificant values.

could be fixed,” both normalized by the total variance. Both coefficients are included here to provide a complete picture of the impact of each parameter. Simulation parameter values were generated using the MATLAB (The MathWorks) `sobolset` function with 1×10^3 and skip 1×10^2 .

Variance-based parameter sensitivity analysis

Table 2 shows that the delay parameters t_{max} and K_I do not have a large effect on the cytosolic Ca^{2+} transient. Although they are necessary to describe the effect of IP₃R-dominated Ca^{2+} dynamics (32), they contribute only a small amount to the variance. Therefore, we decided to fix these parameters in our simulations.

As expected, the coefficients show that cardiac cell Ca^{2+} dynamics during ECC are most highly sensitive to IP₃ concentration ($[IP_3]$) and the maximal flux through each IP₃R

(k_f). The maximal flux k_f has little effect on transient amplitude but large influence on duration and duty cycle, whereas $[IP_3]$ has the greatest effect on the change in amplitude and diastolic Ca^{2+} concentration.

The gating parameters K_C and K_h also influence the cytosolic Ca^{2+} transient. K_h affects the $[Ca^{2+}]$ at which IP₃R channels are inhibited, and K_C affects the $[Ca^{2+}]$ at which IP₃R channels open. We illustrate how these two parameters affect IP₃R open probability, P_{IP_3R} , in Fig. 3. Fig. 3 also shows how $[IP_3]$ affects the relationship between K_C , K_h , $[Ca^{2+}]$, and P_{IP_3R} . It can be seen that with $K_h = 80$ nM, P_{IP_3R} will be close to zero regardless of the values of Ca^{2+} or $[IP_3]$ or K_C . At $K_h = 1.6 \mu M$ and $[IP_3] \geq 5 \mu M$, P_{IP_3R} dependence on K_C and Ca^{2+} becomes apparent. Finally, at $K_h = 3.2 \mu M$, P_{IP_3R} is still dependent on K_C - and Ca^{2+} -values, but $[IP_3]$ does not change P_{IP_3R} significantly.

From this analysis, we determine that for IP₃R channels to be active during ECC, K_h must be sufficiently high that

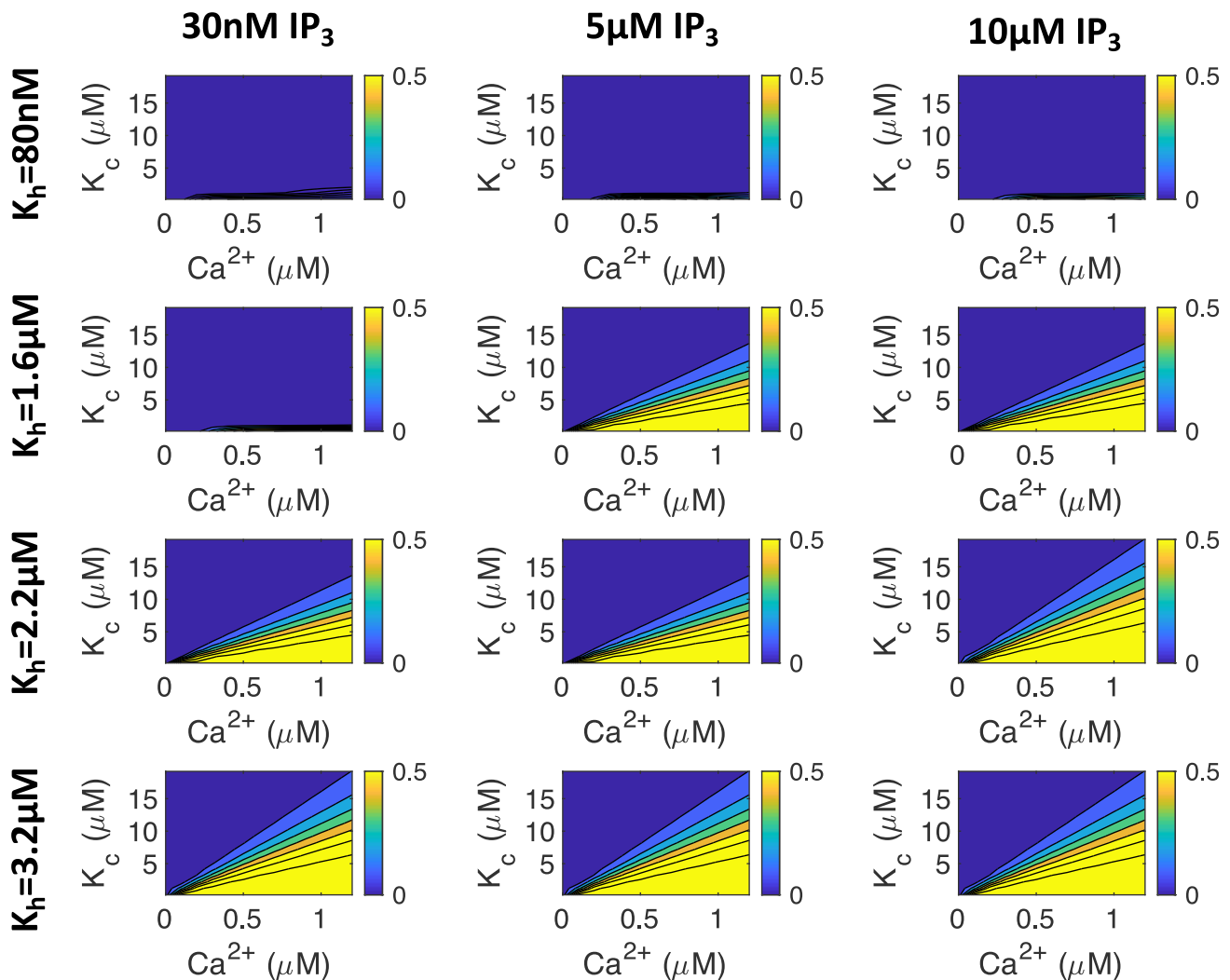


FIGURE 3 The effect of $[Ca^{2+}]$, $[IP_3]$, K_C , and K_h on P_{IP_3R} in the Siekmann-Cao-Sneyd IP₃R model (31,32,46). The colored bars on the side of each plot show the proportion of IP₃R channels that will open for each set of parameters at steady state. Note that IP₃R channels do not open at physiological Ca^{2+} concentrations when K_h is low (i.e., 80 nM or less). In subsequent simulations, we used the value $K_h = 2.2 \mu M$ unless otherwise stated. To see this figure in color, go online.

IP₃R channels are not inhibited at diastolic [Ca²⁺]. Conversely, K_c must be low enough that IP₃R channels are active at Ca²⁺ concentrations below the systolic Ca²⁺ peak. Therefore, in the remainder of this study, we fix K_h at 2.2 μM: high enough to fulfill this condition but low enough that IP₃R channels are still affected by [IP₃]. We report simulation results only within the range of K_c that exhibits experimentally plausible Ca²⁺ transient properties.

With the plausible range of K_h and K_c established, we next show the effect of K_c, k_f, and [IP₃] on the ECC transient.

IP₃ concentration and IP₃R opening behavior have the greatest impact on the Ca²⁺ transient

As summarized in Table 1, different experimental studies suggest different effects of IP₃R activation on the ECC cytosolic Ca²⁺ transient. Fig. 4, A–C show quantitative predictions of how much Ca²⁺ transient properties could be affected by IP₃R activation across a range of [IP₃]- and Ca²⁺-dependent IP₃R gating parameter K_c-values. k_f was fixed at 0.45 μm³ ms⁻¹, and K_h was fixed at 2.2 μM.

The red region in Fig. 4 A corresponds to IP₃R activation parameters that produce the greatest increase in Ca²⁺ amplitude. Noteworthy is that the red region depicts moderate changes in amplitude of ~15%. This region corresponds to K_c-values greater than 4 μM and [IP₃] greater than 2 μM. With K_h set at 2.2 μM, this corresponds to the middle and far-right plots of P_{IP₃R} in Fig. 3. The middle subfigure

shows that with K_c greater than 4 μM, IP₃R channels would open only at Ca²⁺ concentrations greater than the diastolic concentration of ~0.1 μM. The plot also shows that IP₃R channels would remain active at Ca²⁺ greater than the systolic peak concentration of ~1 μM (53). Fig. 4 B further indicates that the increase in peak amplitude is accompanied by an increase in transient duration (FDHM). However, this change may be small, particularly at IP₃ concentrations lower than 1 μM. In Fig. 4 C, it can be seen that the diastolic Ca²⁺ concentration decreases moderately (~10%) in the parameter range in which the amplitude is maximized (Fig. 4 A).

Fig. 4 B shows that FDHM of the Ca²⁺ transient increases whenever IP₃R channels are active. This increase is greater with greater concentrations of IP₃ and with lower values of K_c. Fig. 4 C indicates that K_c and [IP₃] have a similar effect on the diastolic Ca²⁺ concentration except that the location of the red and orange cross predicts a small (~10%) drop in diastolic Ca²⁺. In Fig. 4, A–C, there is little change when [IP₃] is low and K_c is high (*bottom right corner* of each image). This is a regime in which the IP₃R channels barely open in response to ECC transients. For comparison, Fig. S2 shows the same simulations as Fig. 4 at a commonly used experimental pacing frequency of 0.3 Hz, showing similar trends.

To compare our simulation results with the experimental observations summarized in Table 1, we divided the parameter space shown in Fig. 4, A–C into four regions, shown in Fig. 4 D. In the red region, amplitude and FDHM increase. In the orange region, only FDHM increases. In the green

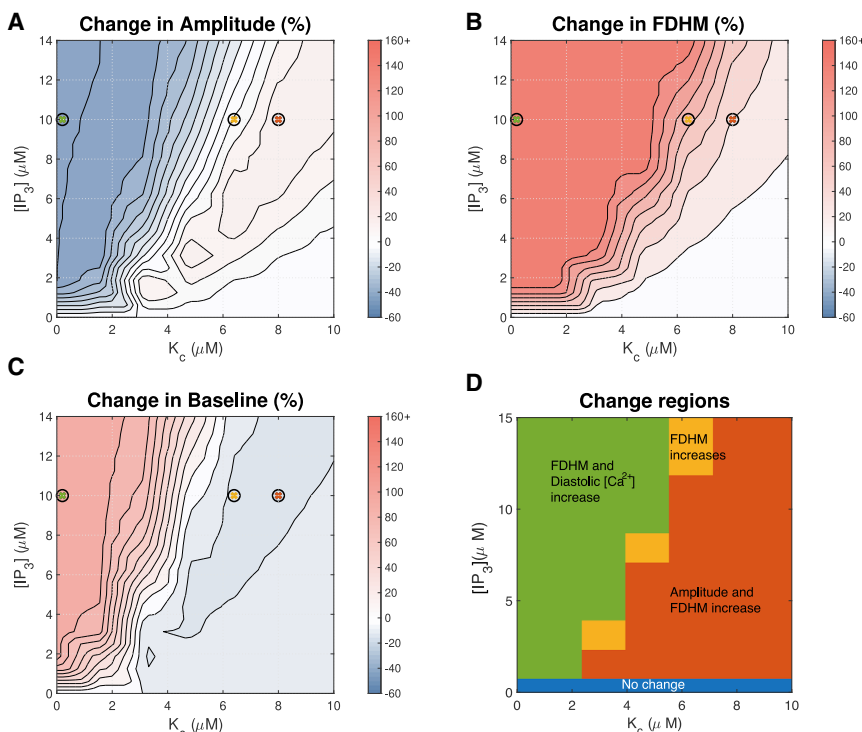


FIGURE 4 Effect of IP₃ concentration and the parameter K_c on the Ca²⁺ transient with pacing frequency 1 Hz. These two parameters, along with maximal IP₃R flux k_f, have the greatest impact when considering the effect of IP₃R activation on the Ca²⁺ transient. To better resolve the range in which FDHM changes, all FDHM increases of 45% and over are shown in the same color. See Fig. 5 for simulated transients at parameters indicated by crosses. We note that for ease of comparison between figures, in this and in subsequent figures, the maximal increase from baseline is cropped at 160%. Changes greater than this threshold are shown in the same color. To see this figure in color, go online.

region, FDHM and diastolic $[Ca^{2+}]$ increase, but amplitude decreases. Comparing to the experimental observation of amplitude increase summarized in Table 1, the red region appears to describe the most plausible parameter range. Fig. 4 D also shows that there is no parameter set in which both amplitude and diastolic Ca^{2+} concentration increase. Furthermore, there is no region in which transients with increased amplitude and decreased duration are observed, as has been reported in ET-1-treated rat ventricular myocyte experiments (54). Finally, with the exception of the blue region in which there is no change, we observe that the FDHM increases in all parameter regimes.

To examine these results further, we investigated model behavior in different regions of Fig. 4 D, shown in Fig. 5 and marked as green, red, and orange crosses in Fig. 4, A–C. Comparing the green cytosolic profiles (corresponding to the green region in Fig. 4 D) and blue cytosolic Ca^{2+} profiles (corresponding to no IP₃R activation) in Fig. 5, we find that IP₃R opening at diastolic Ca^{2+} levels and IP₃R inhibition at Ca^{2+} levels below peak transient concentrations generates a flatter Ca^{2+} transient. This is the result of a gradual depletion of SR Ca^{2+} stores from IP₃R opening. This subsequently leads to lower Ca^{2+} release through RyR and IP₃R channels.

Interestingly, a delayed time to peak is observed with IP₃R activation in all regimes selected. With the reduction in SR load due to IP₃R activation, we find reduced Ca^{2+} flux through RyRs. To maintain or increase Ca^{2+} transient amplitude after activation, the IP₃R channels must compensate for the drop in RyR flux. Because the spike in IP₃R flux is in response to Ca^{2+} release from RyR channels and initial RyR-mediated Ca^{2+}

release is slower with lower SR Ca^{2+} stores, it delays the time between cell stimulation and Ca^{2+} transient peak.

The increase in FDHM of the transient from IP₃R activation apparent in Fig. 4 B can be explained by continued release of Ca^{2+} through IP₃R channels after RyRs have closed in Fig. 5. The slower release through IP₃R channels after RyRs close is a result of a smaller proportion of the channels opening and a decrease in SR Ca^{2+} store load.

Maximal flux through IP₃Rs can increase signal duration

The parameter sensitivity analysis in Table 2 indicates that maximal flux through IP₃Rs (k_f) has the greatest effect on Ca^{2+} transient duration. Therefore, we next examined how increased k_f -values in our model affect the Ca^{2+} transient. Fig. 6, A–C show that for $K_c < 2 \mu M$, increasing k_f above $0.45 \mu m^3 ms^{-1}$ mostly increases transient duration but has only marginal effects on amplitude and baseline. However, for large K_c , the role of k_f in modifying transient shape becomes more noticeable. There is a clear region in which amplitude increases (red region); however, this is more dependent on K_c than k_f . At 1 Hz, there is no value of k_f that reduces transient duration. With IP₃R activation, the transient duration increases, and k_f merely determines by how much. However it is of note that, as shown in Fig. 7, at a lower frequency of 0.3 Hz, when $k_f > 1.2 \mu m^3 ms^{-1}$ and $K_c > 8 \mu M$, there is a decrease in duration of the transient.

To compare simulation results to experimental observations in Table 1, we divided the parameter space shown in

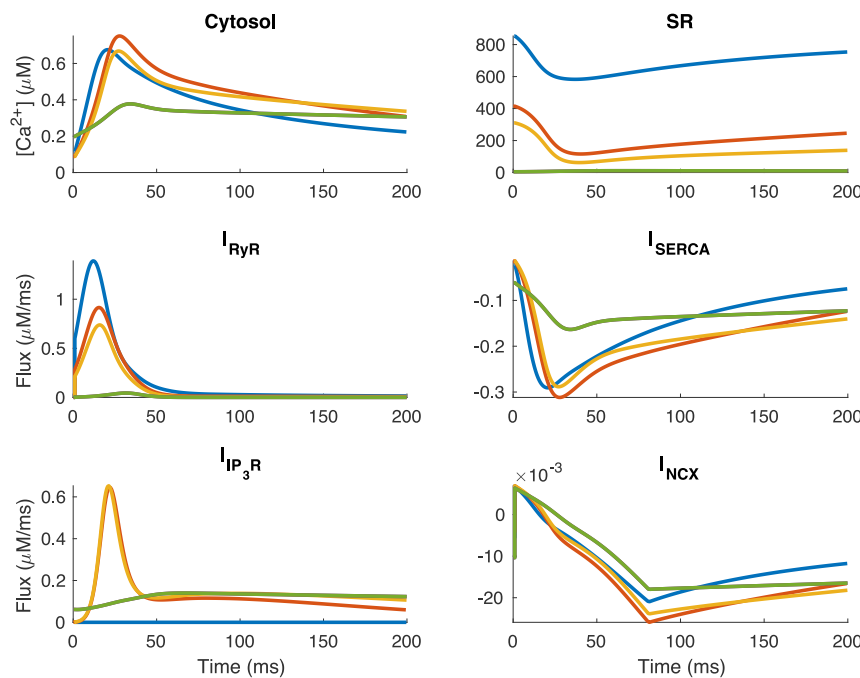


FIGURE 5 Simulated ECC transient and fluxes in the absence (blue) and presence of IP₃, corresponding to low (green), medium (orange), and high (red) values of K_c . With $K_c = 8 \mu M$ (orange), IP₃R channels open only at Ca^{2+} concentrations greater than $0.1 \mu M$. This results in increased peak in cytosolic Ca^{2+} transients and depleted SR Ca^{2+} stores. Parameters here were selected to show absence of IP₃R channels (blue), increased transient amplitude (orange, red), and IP₃R parameterized as described in the original Siekmann-Cao-Sneyd model (green). IP₃ concentration is $10 \mu M$ and pacing frequency 1 Hz in all simulations. The sign of I_{NCX} indicates whether Ca^{2+} is moving into (positive) or out of (negative) the cell. To see this figure in color, go online.

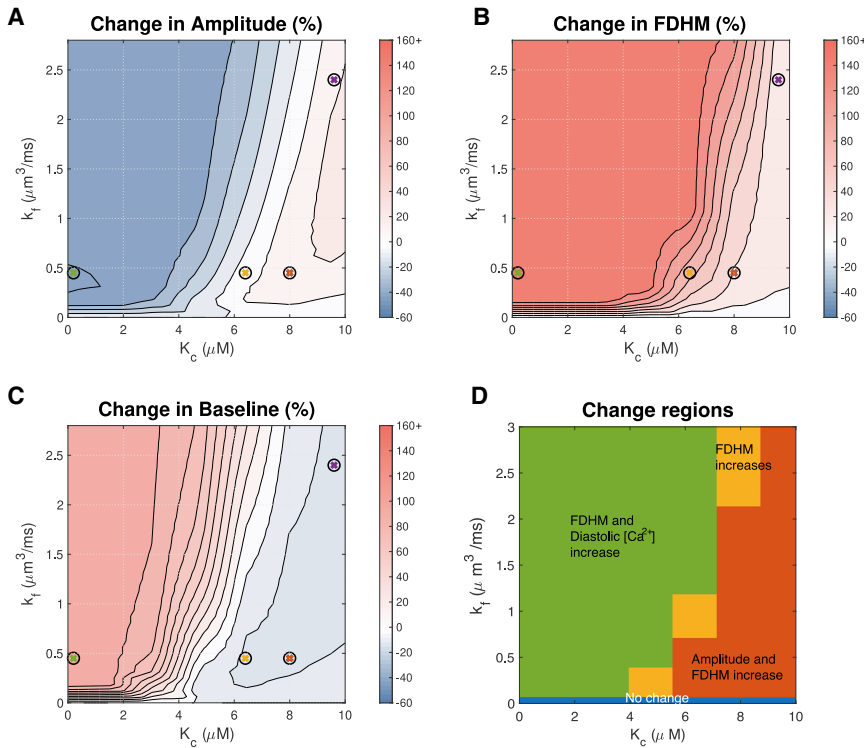


FIGURE 6 Effect of maximal IP₃R flux k_f and the Ca²⁺ sensitivity parameter K_c on the Ca²⁺ transient at 1 Hz. Maximal IP₃R flux has the greatest impact on transient duration. In these simulations, [IP₃] = 10 μM. See Fig. 5 for simulated transients at parameters indicated by crosses. To see this figure in color, go online.

Fig. 6, A–C into three regions, shown in Fig. 6 D. The regions in this figure are consistent with the regions labeled in Fig. 4 D. Fig. 7 D shows similar regions corresponding to simulations at 0.3 Hz. It can be seen that at 0.3 Hz,

$K_c > 8 \mu\text{M}$ and $k_f > 1.2 \mu\text{m}^3 \text{ms}^{-1}$ provide transients with increased amplitude and decreased duration, consistent with the rat ET-1 experiments summarized in Table 1. However, this value of k_f results in an unrealistic flux

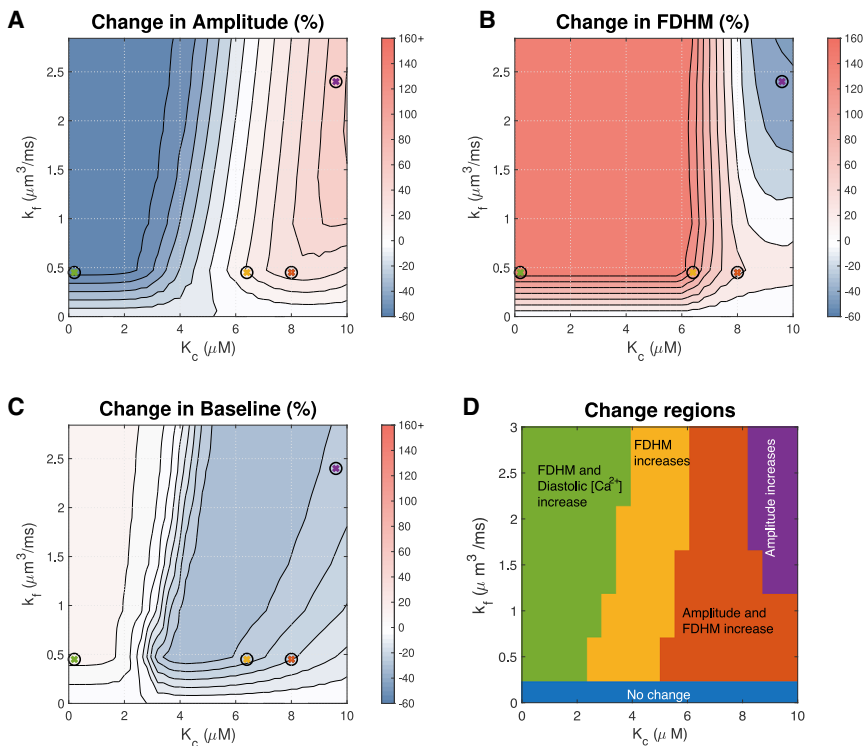


FIGURE 7 Effect of maximal IP₃R flux k_f and the Ca²⁺ sensitivity parameter K_c on the Ca²⁺ transient at 0.3 Hz. Maximal IP₃R flux has the greatest impact on transient duration. In these simulations, [IP₃] = 10 μM. See Fig. S3 for simulated transients at parameter values indicated by crosses. To see this figure in color, go online.

through IP₃R channels. Additionally, *in vivo*, the cell would be paced at a faster frequency, and this result is unlikely without the cell being able to return to resting Ca²⁺. We have not been able to identify a parameter set that would provide a simultaneous increase in both amplitude and diastolic Ca²⁺.

RyR and IP₃R interaction increases the intracellular Ca²⁺ duty cycle

Having established reasonable parameter ranges for IP₃R activation based on the influence on ECC Ca²⁺ transient properties (amplitude, FDHM, and diastolic Ca²⁺), we investigated the possibility that cytosolic Ca²⁺ plays a role in hypertrophic remodeling through changing the duty cycle. Given the timescale involved in hypertrophic remodeling and the signal integration properties of NFAT, the IP₃R-modified cytosolic Ca²⁺ transient could cumulatively encode hypertrophic signaling. Using optogenetic encoding of cytosolic Ca²⁺ transients in HeLa cells, Hannanta-anan and Chow (8) demonstrated that the transcriptional activity of NFAT4 can be upregulated by increasing the cytosolic Ca²⁺ duty cycle. This is a plausible mechanism of signal encoding that is likely to be less susceptible to noise than either amplitude or frequency encoding. Therefore, we examined the cytosolic Ca²⁺ duty cycle as a hypertrophic signaling mechanism.

We calculated the duty cycle for the Ca²⁺ transients in the plausible parameter ranges for IP₃R activation as the ratio

between the area under the Ca²⁺ transient curve and the area of the bounded box defined by the amplitude and period of the Ca²⁺ transient (shown in Fig. 2). Fig. 8 shows the effects of [IP₃], k_f , and K_c on the duty cycle of the cytosolic Ca²⁺ transient. The figure shows that the Ca²⁺ duty cycle increases with IP₃R activation across the broad parameter range shown.

NFAT activation increases with an increase in calcium duty cycle

Having established that IP₃R activation results in increased calcium transient duty cycle, we coupled the model of cytosolic ARVM calcium dynamics to the model of NFAT activation developed by Cooling et al. (50). We then tested the effect of varying IP₃ concentration over a range of IP₃R parameter values on the proportion of dephosphorylated nuclear NFAT compared with that in the phosphorylated inactive state in the cytosol (Fig. 9). These simulation data clearly show that increased IP₃ and alteration in the Ca²⁺ transient duty cycle positively influence NFAT activation and thus provides a mechanism to couple IP₃-induced Ca²⁺ release and activation of hypertrophic gene expression.

DISCUSSION

Here, we have presented what is, to our knowledge, the first modeling study to investigate the effect of IP₃R channel activity on the cardiac ECC Ca²⁺ transient and possible

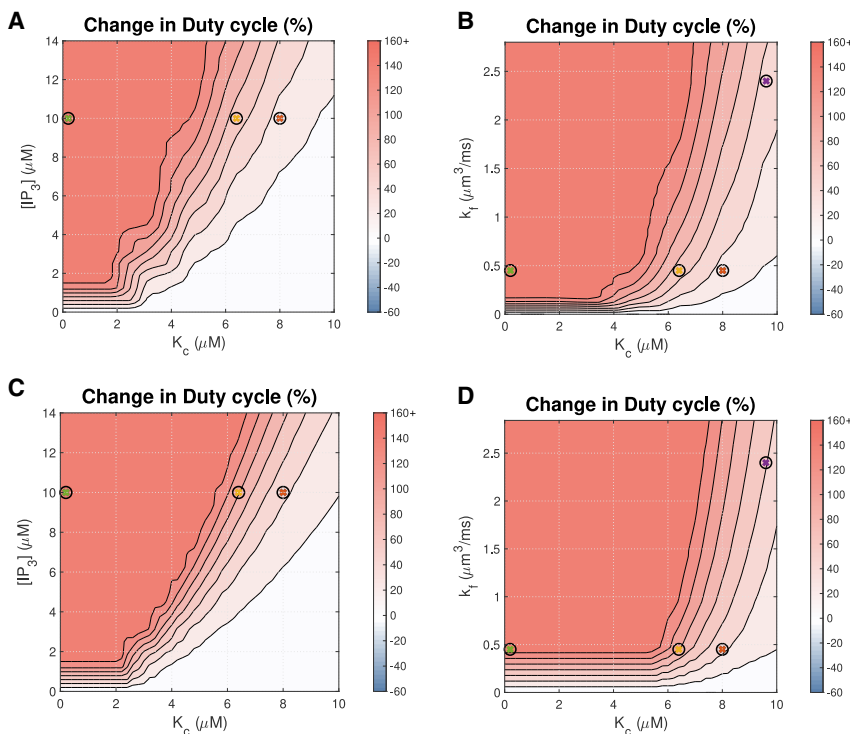


FIGURE 8 Effects on the Ca²⁺ transient duty cycle of (A) IP₃ concentration and the Ca²⁺ sensitivity parameter K_c with pacing frequency 1 Hz, (B) maximal IP₃R flux k_f and K_c with pacing frequency 1 Hz, (C) IP₃ concentration and K_c with pacing frequency 0.3 Hz, and (D) maximal IP₃R flux k_f and K_c at pacing frequency 0.3 Hz. The color bar indicates the percent change from a simulation run with identical parameters but no IP₃R channels. The colored crosses indicate the parameters used for the corresponding plots in Fig. 5. Hannanta-anan and Chow (8) report a transcription rate increase of ~30% with a duty cycle increase of 50% in Fig. 2 of their work. The duty cycle of the Ca²⁺ transient when IP₃Rs are inactive is 0.127. To see this figure in color, go online.

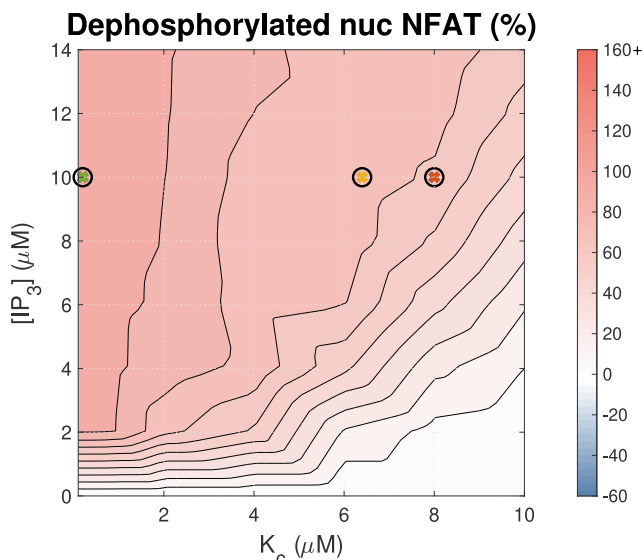


FIGURE 9 Effect of $[IP_3]$ and K_c on the concentration of dephosphorylated nuclear NFAT ($NFAT_n$). Simulations were paced at 1 Hz. The color bar indicates the percent change from a simulation run with identical parameters but no IP_3 . To see this figure in color, go online.

information encoding mechanisms. We extended a well-established model of the ECC Ca^{2+} transient by Hinch et al. (14) to include a model of IP_3R activation and Ca^{2+} release. The model, upon IP_3R activation, simulates the influence of IP_3R activation on Ca^{2+} transients in nonhypertrophic adult rat left ventricular cardiac myocytes.

Parameter sensitivity analysis (Table 2) showed the maximal IP_3 -induced Ca^{2+} release through individual IP_3R (k_f) had the greatest influence on the Ca^{2+} transient duration and duty cycle. $[IP_3]$ had the biggest influence on the Ca^{2+} amplitude and diastolic Ca^{2+} concentration. We found that under fixed maximal IP_3R flux, $k_f = 0.45 \mu M^3 ms^{-1}$, IP_3R activation increases the duration of the Ca^{2+} transient, but Ca^{2+} amplitude is IP_3 dependent. The Ca^{2+} transient duration can be reduced only by increasing k_f to physiologically unrealistic values.

The finding that the Ca^{2+} transient duty cycle increases with $[IP_3]$ (see Fig. 8) provides a plausible explanation for the mechanism by which IP_3 -dependent Ca^{2+} release from IP_3Rs can enhance pro-hypertrophic NFAT activity.

Does IP_3 -induced Ca^{2+} release modify the ECC transient?

Figs. 4, 6 and 7 show that IP_3Rs can influence the ECC Ca^{2+} transient and that the effect is dependent on the IP_3R properties and IP_3 concentration. Our model simulations predict that Ca^{2+} transient amplitude increases $\sim 15\%$ when IP_3R properties are such that IP_3Rs remain inhibited from opening at diastolic Ca^{2+} but release Ca^{2+} once RyRs are activated and remain open when Ca^{2+} concentration is above $1 \mu M$. The IP_3R parameter combination marked by a red

cross in the contour plots is a representative example of this type of effect of IP_3Rs . There is also a narrow parameter range at $[IP_3]$ of $10 \mu M$ ($K_h = 2.2 \mu M$, $K_c = 6 \mu M$) in which the amplitude does not change more than 5% (see Fig. 4). The orange cross marks an example of IP_3R effects in this parameter range. These simulation predictions are consistent with the experimental studies that either show increased amplitude or no change in amplitude (Table 1).

Model simulations predict that IP_3R activation only increases diastolic $[Ca^{2+}]$ when IP_3Rs are open at resting $[Ca^{2+}]$ of $\sim 0.1 \mu M$ (see Fig. 4 D). Harzheim et al. (17) reported no measurable differences in diastolic $[Ca^{2+}]$ between ARVMs stimulated with an agonist known to induce hypertrophy in healthy ARVMs and those treated with a saline buffer (although effects have been observed in disease ventricular cardiomyocytes and atrial cardiomyocytes). Examination of simulated Ca^{2+} transients within a regime that results in diastolic $[Ca^{2+}]$ increase (green traces in Fig. 5) shows that the transients do not resemble any of the observed experimental measurements in the literature. Therefore, the comparison of model simulations and experimental measurements of diastolic $[Ca^{2+}]$ and Ca^{2+} transient amplitude suggest that the most likely regime of IP_3R activation lies between the orange and red regions in Fig. 4 D. Using these comparisons, we propose that IP_3R activation makes modest changes to the ECC Ca^{2+} transient that are often hidden within the measurement variability in experiments.

The biological significance of the duty cycle

We showed that although amplitude, duration, and diastolic Ca^{2+} can increase or decrease depending on IP_3R parameter values and pacing frequency, the duty cycle, as defined by Hannanta-anan and Chow (8), always increases with IP_3 , consistent with effects seen in (21). The implication of this observation is that IP_3R activation is sufficient to provide a signal to drive NFAT nuclear translocation and hence hypertrophic gene expression in the manner described by Hannanta-anan and Chow (8).

Hannanta-anan and Chow (8) found that when comparing Ca^{2+} oscillations of the same amplitude, oscillations with greater duty cycle had a greater effect on NFAT dephosphorylation and translocation to the nucleus. In their study, duty cycle, γ , was calculated as the area under the curve, U , divided by the maximal area under the curve (for Ca^{2+} oscillations of the same amplitude, A , and period of oscillation, T), i.e., $\gamma = U/AT$ (see Fig. 2 A). An alternative definition is $\gamma = \Delta/T$, where Δ is the transient duration and T the period of oscillation. This alternate formulation is used by Tomida et al. (37) and Salazar et al. (55) but is less well defined for analog signals. The duty cycle in Fig. 8 was calculated using the former definition. This can be compared with the latter definition when remembering that duty cycle will now vary with FDHM (Figs. 4 C and 6 C).

The duty cycle in this system essentially reflects the fraction of each period of the Ca²⁺ cycle for which cytosolic Ca²⁺ is sufficiently elevated to affect the downstream proteins in the CnA/NFAT signaling pathway. The greater sensitivity of NFAT to Ca²⁺ oscillations with sustained elevation in intracellular Ca²⁺ is well established (19,38,56). Although it is difficult to determine where this threshold is, NFAT is a Ca²⁺ integrator, and a clear correlation has been found between Ca²⁺ duty cycle and NFAT activation (8). Increasing duty cycle increases the time NFAT spends in the dephosphorylated state, which is required to both enter and maintain it in the nucleus and hence affects transcription (57); NFAT responds to changes in duty cycle while being insensitive to both amplitude and frequency changes. We see in simulations too that the proportion of NFAT that is in the dephosphorylated nuclear state is highest when the duty cycle of the Ca²⁺ transient is high (Figs. 8 and 9).

In experiments, IP₃ stimulation has been shown to lead to an increase in systolic Ca²⁺ in cardiac cells, but a significant change in duration has not been reported (although as in Harzheim et al. (17) and Proven et al. (21), increased spontaneous calcium transients are observed that could function to prolong the duration of the Ca²⁺ transient). Based on the definition of the duty cycle presented in Hannanta-anan and Chow (8), there is a negative effect on duty cycle, and hence NFAT activation, when Ca²⁺ transient amplitude is increased. However, within the physiologically plausible parameter range, we find that simulations with increased Ca²⁺ transient amplitude also have increased transient duration. We postulate that NFAT may be responsive to the Ca²⁺ transient through the latter definition of the duty cycle—i.e., the duration of time that Ca²⁺ is elevated over a threshold divided by the period. This is more consistent with both the biological mechanism and the potential increase in peak Ca²⁺ concentration in the hypertrophic pathway, which may be a side effect of a corresponding increase in duration over this threshold. Further research, both theoretical and experimental, is required to determine the validity of this assumption.

Fig. 9 shows a strong correlation between [Ca²⁺]-dependent NFAT activation and Ca²⁺ transient duty cycle in the Cooling et al. (50) model; the correspondence between Figs. 8 A and 9 is striking. A caveat, however, is that the original Cooling et al. (50) study showed that the NFAT model is also sensitive to any average increase in cytosolic calcium. Therefore, although increasing Ca²⁺ transient duty cycle is shown to be sufficient for NFAT activation in this model, further experimental validation is required to confirm this mechanism in cardiomyocytes.

Experimental evidence of an IP₃-induced increase in calcium duty cycle?

An increase in duty cycle without an increase in frequency requires an increase in transient duration. Although this in-

crease is observed in our simulations for a broad range of parameter values, it has not, however, been reported in experiments involving IP₃ stimulation. The possible reasons for this are many and varied; however, as discussed earlier, using different IP₃ concentrations to those that occur in vivo may result in different effects on the shape of the Ca²⁺ oscillations, leading to inconsistent observations. Furthermore, small variations in Ca²⁺ concentrations may not be experimentally discernible or may be hidden by the effect of Ca²⁺-sensitive dyes (58). A small but prolonged variation in transient duration can produce a comparatively large change in duty cycle. Hence, it remains to be confirmed experimentally whether IP₃R-dependent Ca²⁺ flux does indeed lead to an increased Ca²⁺ duty cycle in cardiomyocytes.

Limitations of study

In this study, we have considered generation of voltage-driven cytosolic Ca²⁺ transients using deterministic models of each ion channel in a compartmental model. There are several physiological features of cardiomyocyte Ca²⁺ dynamics that are not represented and hence not considered in this approach. In particular, our model does not represent any of the stochastic events associated with IP₃R channels. Further modeling of combined stochastic channel gating may be necessary to elucidate the entire impact of IP₃R interaction with the cytosolic Ca²⁺ machinery. Although cell structure is known to play a role in cardiac Ca²⁺ dynamics (59–61), effects beyond the synchronizing function of the dyad are not considered in this compartmental study. Furthermore, we have not considered the spatial IP₃R distribution. Our model is developed primarily using parameters fitted by (14) and (32) and makes no distinction between IP₃R channels located within or outside the dyad (62,63). These and other structural features of the cell could alter the Ca²⁺ available to regulate IP₃R channels and may be detected in the Ca²⁺ transient. Distinct effects of IP₃ signaling in the cytosol and the nucleus are also not considered. Cytosolic Ca²⁺ is thought to promote translocation of NFAT into the nucleus, whereas nuclear Ca²⁺ maintains it there (16). We have only investigated the former role for Ca²⁺ signaling within the CnA/NFAT pathway.

We have explored model behavior at pacing frequencies of 1 and 0.3 Hz rather than higher, more physiological frequencies, primarily because the majority of parameters were derived from in vitro experiments conducted at room temperature. Extrapolation of parameters, and hence model behavior, to in vivo temperature and correspondingly higher pacing frequency remains challenging. Therefore, model predictions must be interpreted cautiously in relation to higher pacing frequencies.

Additionally, not all components of this signaling pathway have been considered in this study. Ca²⁺/

calmodulin-dependent kinases II and Class IIa histone deacetylases, for example, are both known Ca^{2+} -mediated components of the hypertrophic pathway that are activated by IP_3 signaling (64) but are not included. Here, we have focused only on the impact of IP_3R activation on the cytosolic Ca^{2+} dynamics and how this relates to the mechanism of NFAT activation. To explore broader context for IP_3 -mediated hypertrophic signaling, it remains to couple this model to upstream events, including models of IP_3 production through activation of cell membrane receptors (65,66). This would allow the profile and extent of the rise in IP_3 concentration due to the activation of the hypertrophic pathway in cardiomyocytes to be determined. We have focused on the effect of an elevated IP_3 concentration of $10\ \mu\text{M}$ because many experimental studies on the effect of IP_3 on Ca^{2+} dynamics use saturating $[\text{IP}_3]$. However, Remus et al. (67) found stimulation of adult cat ventricular myocytes with $100\ \text{nM}$ ET-1 induced a cell-averaged increase in IP_3 concentration of only $10\ \text{nM}$, indicating a much lower concentration than used in experiments. This, together with known differences between species, suggests the IP_3 concentration detected by IP_3R receptors in ARVMs in vivo could be lower than the simulated $10\ \mu\text{M}$. However, we note qualitatively similar effects on the Ca^{2+} transient in parameter regimes with lower $[\text{IP}_3]$ in our model (Figs. 4 and S2), albeit with more modest effects on the transient shape. Additionally, ET-1 receptors are localized to t-tubule membranes (68), so IP_3 may be generated very close to IP_3R channels (63,69), increasing the concentration they detect.

Finally, IP_3R -induced Ca^{2+} release is a part of a larger hypertrophic signaling network. It remains to couple this model to other signaling pathways involved in bringing about hypertrophic remodeling (70). How cytosolic Ca^{2+} interacts with nuclear Ca^{2+} in regulation of NFAT nuclear residence and activity also remains to be determined.

CONCLUSIONS

The sensitivity of NFAT translocation to the Ca^{2+} duty cycle demonstrated by Hannanta-anan and Chow (8) raises the question as to whether IP_3R flux can increase the Ca^{2+} duty cycle in cardiomyocytes during hypertrophic signaling. Here, we have shown, using mathematical modeling, that an increase in cytosolic Ca^{2+} transient duration can occur after addition of IP_3 , and furthermore, that this increase is sufficient to increase NFAT activation. Together, these results suggest a plausible mechanism for hypertrophic signaling via IP_3R activation in cardiomyocytes. Although it cannot be ruled out that a significant role is played by components of this pathway that are not considered here, the computational evidence provided in this study, along with the previous experimental findings, suggests encoding of the hypertrophic signal through alteration of the duration of cytosolic Ca^{2+} oscillations to be a feasible mechanism for IP_3 -dependent hypertrophic signaling.

SUPPORTING MATERIAL

Supporting Material can be found online at <https://doi.org/10.1016/j.bpj.2020.08.001>.

AUTHOR CONTRIBUTIONS

E.J.C., V.R., H.L.R., C.S., and G.B. conceived of the study. E.J.C. and V.R. supervised the project. H.H., A.T., V.R., and E.J.C. developed the modeling approach. H.H. implemented the simulations. H.L.R., C.S., and G.B. provided critical feedback. All authors contributed to writing the manuscript.

ACKNOWLEDGMENTS

This research was supported in part by the Australian Government through the Australian Research Council Discovery Projects funding scheme (project DP170101358). H.L.R. wishes to acknowledge financial support from the Research Foundation Flanders through project grant G08861N and Odysseus programme grant 90663.

SUPPORTING CITATIONS

References (71,72) appear in the Supporting Material.

REFERENCES

- Berridge, M. J., M. D. Bootman, and H. L. Roderick. 2003. Calcium signalling: dynamics, homeostasis and remodelling. *Nat. Rev. Mol. Cell Biol.* 4:517–529.
- Clapham, D. E. 2007. Calcium signaling. *Cell.* 131:1047–1058.
- Berridge, M. J. 1997. The AM and FM of calcium signalling. *Nature.* 386:759–760.
- Berridge, M. J. 2006. Calcium microdomains: organization and function. *Cell Calcium.* 40:405–412.
- Bootman, M. D., C. Fearnley, ..., H. L. Roderick. 2009. An update on nuclear calcium signalling. *J. Cell Sci.* 122:2337–2350.
- Purvis, J. E., and G. Lahav. 2013. Encoding and decoding cellular information through signaling dynamics. *Cell.* 152:945–956.
- Uzhachenko, R., A. Shanker, and G. Dupont. 2016. Computational properties of mitochondria in T cell activation and fate. *Open Biol.* 6:160192.
- Hannanta-Anan, P., and B. Y. Chow. 2016. Optogenetic control of calcium oscillation waveform defines NFAT as an integrator of calcium load. *Cell Syst.* 2:283–288.
- Roderick, H. L., D. R. Higazi, ..., M. D. Bootman. 2007. Calcium in the heart: when it's good, it's very very good, but when it's bad, it's horrid. *Biochem. Soc. Trans.* 35:957–961.
- Hohendanner, F., J. T. Maxwell, and L. A. Blatter. 2015. Cytosolic and nuclear calcium signaling in atrial myocytes: IP_3 -mediated calcium release and the role of mitochondria. *Channels (Austin).* 9:129–138.
- Zinn, M., S. West, and B. Kuhn. 2018. Mechanisms of cardiac hypertrophy. In *Heart Failure in the Child and Young Adult*. J. L. Jefferies, A. C. Chang, J. W. Rossano, R. E. Shaddy, and J. A. Towbin, eds. Academic Press, pp. 51–58.
- Tham, Y. K., B. C. Bernardo, ..., J. R. McMullen. 2015. Pathophysiology of cardiac hypertrophy and heart failure: signaling pathways and novel therapeutic targets. *Arch. Toxicol.* 89:1401–1438.
- Gilbert, G., K. Demydenko, ..., H. L. Roderick. 2020. Calcium signaling in cardiomyocyte function. *Cold Spring Harb. Perspect. Biol.* 12:035428.
- Hinch, R., J. L. Greenstein, ..., R. L. Winslow. 2004. A simplified local control model of calcium-induced calcium release in cardiac ventricular myocytes. *Biophys. J.* 87:3723–3736.

15. Vierheller, J., W. Neubert, ..., N. Chamakuri. 2015. A multiscale computational model of spatially resolved calcium cycling in cardiac myocytes: from detailed cleft dynamics to the whole cell concentration profiles. *Front. Physiol.* 6:255.
16. Higazi, D. R., C. J. Fearnley, ..., H. L. Roderick. 2009. Endothelin-1-stimulated InsP3-induced Ca²⁺ release is a nexus for hypertrophic signaling in cardiac myocytes. *Mol. Cell.* 33:472–482.
17. Harzheim, D., M. Movassagh, ..., H. L. Roderick. 2009. Increased InsP3Rs in the junctional sarcoplasmic reticulum augment Ca²⁺ transients and arrhythmias associated with cardiac hypertrophy. *Proc. Natl. Acad. Sci. USA.* 106:11406–11411.
18. Nakayama, H., I. Bodi, ..., J. D. Molkentin. 2010. The IP3 receptor regulates cardiac hypertrophy in response to select stimuli. *Circ. Res.* 107:659–666.
19. Rinne, A., N. Kapur, ..., L. A. Blatter. 2010. Isoform- and tissue-specific regulation of the Ca(2+)-sensitive transcription factor NFAT in cardiac myocytes and heart failure. *Am. J. Physiol. Heart Circ. Physiol.* 298:H2001–H2009.
20. Signore, S., A. Sorrentino, ..., M. Rota. 2013. Inositol 1, 4, 5-trisphosphate receptors and human left ventricular myocytes. *Circulation.* 128:1286–1297.
21. Proven, A., H. L. Roderick, ..., M. D. Bootman. 2006. Inositol 1,4,5-trisphosphate supports the arrhythmogenic action of endothelin-1 on ventricular cardiac myocytes. *J. Cell Sci.* 119:3363–3375.
22. Domeier, T. L., A. V. Zima, ..., L. A. Blatter. 2008. IP3 receptor-dependent Ca²⁺ release modulates excitation-contraction coupling in rabbit ventricular myocytes. *Am. J. Physiol. Heart Circ. Physiol.* 294:H596–H604.
23. Ljubojevic, S., S. Radulovic, ..., B. Pieske. 2014. Early remodeling of perinuclear Ca²⁺ stores and nucleoplasmic Ca²⁺ signaling during the development of hypertrophy and heart failure. *Circulation.* 130:244–255.
24. Olivares-Florez, S., M. Czolbe, ..., O. Ritter. 2018. Nuclear calcineurin is a sensor for detecting Ca²⁺ release from the nuclear envelope via IP₃R. *J. Mol. Med. (Berl).* 96:1239–1249.
25. Smyrnias, I., N. Goodwin, ..., H. L. Roderick. 2018. Contractile responses to endothelin-1 are regulated by PKC phosphorylation of cardiac myosin binding protein-C in rat ventricular myocytes. *J. Mol. Cell. Cardiol.* 117:1–18.
26. Harzheim, D., A. Talasila, ..., H. L. Roderick. 2010. Elevated InsP3R expression underlies enhanced calcium fluxes and spontaneous extrasystolic calcium release events in hypertrophic cardiac myocytes. *Channels (Austin).* 4:67–71.
27. Foskett, J. K., C. White, ..., D.-O. D. Mak. 2007. Inositol trisphosphate receptor Ca²⁺ release channels. *Physiol. Rev.* 87:593–658.
28. Ramos-Franco, J., D. Bare, ..., G. Mignery. 2000. Single-channel function of recombinant type 2 inositol 1,4, 5-trisphosphate receptor. *Biophys. J.* 79:1388–1399.
29. Siekmann, I., J. Sneyd, and E. J. Crampin. 2014. Statistical analysis of modal gating in ion channels. *Proc. R. Soc. A Math. Phys. Eng. Sci.* 470:20140030.
30. Siekmann, I., P. Cao, ..., E. J. Crampin. 2019. Data-driven modelling of the inositol trisphosphate receptor (IP₃R) and its role in calcium-induced calcium release (CICR). In *Computational Glioscience*. M. De Pittá and H. Berry, eds. Springer International Publishing, pp. 39–68.
31. Cao, P., X. Tan, ..., J. Sneyd. 2014. A deterministic model predicts the properties of stochastic calcium oscillations in airway smooth muscle cells. *PLoS Comput. Biol.* 10:e1003783.
32. Sneyd, J., J. M. Han, ..., D. I. Yule. 2017. On the dynamical structure of calcium oscillations. *Proc. Natl. Acad. Sci. USA.* 114:1456–1461.
33. Siekmann, I., J. Sneyd, and E. J. Crampin. 2012. MCMC can detect nonidentifiable models. *Biophys. J.* 103:2275–2286.
34. Terkildsen, J. R., S. Niederer, ..., N. P. Smith. 2008. Using Physiome standards to couple cellular functions for rat cardiac excitation-contraction. *Exp. Physiol.* 93:919–929.
35. Wilkins, B. J., L. J. De Windt, ..., J. D. Molkentin. 2002. Targeted disruption of NFATc3, but not NFATc4, reveals an intrinsic defect in calcineurin-mediated cardiac hypertrophic growth. *Mol. Cell. Biol.* 22:7603–7613.
36. Molkentin, J. D., J. R. Lu, ..., E. N. Olson. 1998. A calcineurin-dependent transcriptional pathway for cardiac hypertrophy. *Cell.* 93:215–228.
37. Tomida, T., K. Hirose, ..., M. Iino. 2003. NFAT functions as a working memory of Ca²⁺ signals in decoding Ca²⁺ oscillation. *EMBO J.* 22:3825–3832.
38. Colella, M., F. Grisan, ..., T. Pozzan. 2008. Ca²⁺ oscillation frequency decoding in cardiac cell hypertrophy: role of calcineurin/NFAT as Ca²⁺ signal integrators. *Proc. Natl. Acad. Sci. USA.* 105:2859–2864.
39. Saucerman, J. J., and D. M. Bers. 2008. Calmodulin mediates differential sensitivity of CaMKII and calcineurin to local Ca²⁺ in cardiac myocytes. *Biophys. J.* 95:4597–4612.
40. Ulrich, J. D., M.-S. Kim, ..., Y. M. Usachev. 2012. Distinct activation properties of the nuclear factor of activated T-cells (NFAT) isoforms NFATc3 and NFATc4 in neurons. *J. Biol. Chem.* 287:37594–37609.
41. Yissachar, N., T. Sharar Fischler, ..., N. Friedman. 2013. Dynamic response diversity of NFAT isoforms in individual living cells. *Mol. Cell.* 49:322–330.
42. Kar, P., G. R. Mirams, ..., A. B. Parekh. 2016. Control of NFAT isoform activation and NFAT-dependent gene expression through two coincident and spatially segregated intracellular Ca²⁺ signals. *Mol. Cell.* 64:746–759.
43. Pandit, S. V., W. R. Giles, and S. S. Demir. 2003. A mathematical model of the electrophysiological alterations in rat ventricular myocytes in type-I diabetes. *Biophys. J.* 84:832–841.
44. Wagner, J., and J. Keizer. 1994. Effects of rapid buffers on Ca²⁺ diffusion and Ca²⁺ oscillations. *Biophys. J.* 67:447–456.
45. Moschella, M. C., and A. R. Marks. 1993. Inositol 1,4,5-trisphosphate receptor expression in cardiac myocytes. *J. Cell Biol.* 120:1137–1146.
46. Siekmann, I., L. E. Wagner, II, ..., J. Sneyd. 2012. A kinetic model for type I and II IP₃R accounting for mode changes. *Biophys. J.* 103:658–668.
47. Ramos-Franco, J., M. Fill, and G. A. Mignery. 1998. Isoform-specific function of single inositol 1,4,5-trisphosphate receptor channels. *Biophys. J.* 75:834–839.
48. Zima, A. V., E. Bovo, ..., L. A. Blatter. 2010. Ca²⁺ spark-dependent and -independent sarcoplasmic reticulum Ca²⁺ leak in normal and failing rabbit ventricular myocytes. *J. Physiol.* 588:4743–4757.
49. Blanch I Salvador, J., and M. Egger. 2018. Obstruction of ventricular Ca²⁺-dependent arrhythmogenicity by inositol 1,4,5-trisphosphate-triggered sarcoplasmic reticulum Ca²⁺ release. *J. Physiol.* 596:4323–4340.
50. Cooling, M. T., P. Hunter, and E. J. Crampin. 2009. Sensitivity of NFAT cycling to cytosolic calcium concentration: implications for hypertrophic signals in cardiac myocytes. *Biophys. J.* 96:2095–2104.
51. Jansen, M. J. W. 1999. Analysis of variance designs for model output. *Comput. Phys. Commun.* 117:35–43.
52. Saltelli, A., P. Annoni, ..., S. Tarantola. 2010. Variance based sensitivity analysis of model output. Design and estimator for the total sensitivity index. *Comput. Phys. Commun.* 181:259–270.
53. Greenstein, J. L., and R. L. Winslow. 2002. An integrative model of the cardiac ventricular myocyte incorporating local control of Ca²⁺ release. *Biophys. J.* 83:2918–2945.
54. Moravec, C. S., E. E. Reynolds, ..., M. Bond. 1989. Endothelin is a positive inotropic agent in human and rat heart in vitro. *Biochem. Biophys. Res. Commun.* 159:14–18.
55. Salazar, C., A. Z. Politi, and T. Höfer. 2008. Decoding of calcium oscillations by phosphorylation cycles: analytic results. *Biophys. J.* 94:1203–1215.
56. Dolmetsch, R. E., R. S. Lewis, ..., J. I. Healy. 1997. Differential activation of transcription factors induced by Ca²⁺ response amplitude and duration. *Nature.* 386:855–858.

57. Feske, S., R. Draeger, ..., A. Rao. 2000. The duration of nuclear residence of NFAT determines the pattern of cytokine expression in human SCID T cells. *J. Immunol.* 165:297–305.
58. Sparrow, A. J., K. Sievert, ..., M. J. Daniels. 2019. Measurement of myofilament-localized calcium dynamics in adult cardiomyocytes and the effect of hypertrophic cardiomyopathy mutations. *Circ. Res.* 124:1228–1239.
59. Gaur, N., and Y. Rudy. 2011. Multiscale modeling of calcium cycling in cardiac ventricular myocyte: macroscopic consequences of microscopic dyadic function. *Biophys. J.* 100:2904–2912.
60. Rajagopal, V., G. Bass, ..., C. Soeller. 2015. Examination of the effects of heterogeneous organization of RYR clusters, myofibrils and mitochondria on Ca²⁺ release patterns in cardiomyocytes. *PLoS Comput. Biol.* 11:e1004417–e1004431.
61. Ladd, D., A. Tilūnaitė, ..., V. Rajagopal. 2019. Assessing cardiomyocyte excitation-contraction coupling site detection from live cell imaging using a structurally-realistic computational model of calcium release. *Front. Physiol.* 10:1263.
62. Mohler, P. J., J.-J. Schott, ..., V. Bennett. 2003. Ankyrin-B mutation causes type 4 long-QT cardiac arrhythmia and sudden cardiac death. *Nature.* 421:634–639.
63. Mohler, P. J., J. Q. Davis, and V. Bennett. 2005. Ankyrin-B coordinates the Na/K ATPase, Na/Ca exchanger, and InsP3 receptor in a cardiac T-tubule/SR microdomain. *PLoS Biol.* 3:e423.
64. Wu, X., T. Zhang, ..., D. M. Bers. 2006. Local InsP3-dependent perinuclear Ca²⁺ signaling in cardiac myocyte excitation-transcription coupling. *J. Clin. Invest.* 116:675–682.
65. Cooling, M., P. Hunter, and E. J. Crampin. 2007. Modeling hypertrophic IP3 transients in the cardiac myocyte. *Biophys. J.* 93:3421–3433.
66. Cooling, M. T., P. J. Hunter, and E. J. Crampin. 2008. Modelling biological modularity with CellML. *IET Syst. Biol.* 2:73–79.
67. Remus, T. P., A. V. Zima, ..., G. A. Mignery. 2006. Biosensors to measure inositol 1,4,5-trisphosphate concentration in living cells with spatiotemporal resolution. *J. Biol. Chem.* 281:608–616.
68. Boivin, B., D. Chevalier, ..., B. G. Allen. 2003. Functional endothelin receptors are present on nuclei in cardiac ventricular myocytes. *J. Biol. Chem.* 278:29153–29163.
69. Escobar, M., C. Cardenas, ..., C. Franzini-Armstrong. 2011. Structural evidence for perinuclear calcium microdomains in cardiac myocytes. *J. Mol. Cell. Cardiol.* 50:451–459.
70. Ryall, K. A., D. O. Holland, ..., J. J. Saucerman. 2012. Network reconstruction and systems analysis of cardiac myocyte hypertrophy signaling. *J. Biol. Chem.* 287:42259–42268.
71. Yu, T., C. M. Lloyd, ..., P. M. F. Nielsen. 2011. The physiome model repository 2. *Bioinformatics.* 27:743–744.
72. Thomas, D., S. C. Tovey, ..., P. Lipp. 2000. A comparison of fluorescent Ca²⁺ indicator properties and their use in measuring elementary and global Ca²⁺ signals. *Cell Calcium.* 28:213–223.
73. Escobar, A. L., C. G. Perez, ..., J. Ramos-Franco. 2012. Role of inositol 1,4,5-trisphosphate in the regulation of ventricular Ca(2+) signaling in intact mouse heart. *J. Mol. Cell. Cardiol.* 53:768–779.